Focused SAR Image Formation of Moving Targets based on Doppler Parameter Estimation

Carlo Noviello, Gianfranco Fornaro, *Senior Member, IEEE,*

and Marco Martorella, *Senior Member, IEEE,*

Abstract

The present work addresses the problem of focusing moving target in SAR images. This task is here solved by using an Inverse Synthetic Aperture Radar (ISAR) technique. The ISAR technique performs an autofocus procedure by implementing exhaustive search algorithms, improved by classical convex optimization, of functions based on image contrast or entropy. In this work, we discuss the possibility to perform an autofocus ISAR technique by exploiting the estimation of the target Doppler parameters: namely the Doppler centroid and the Doppler rate, which are related to the target motion parameters. The present algorithm is based on the re-use of efficient autofocus approaches that are classically used in direct SAR imaging. The effectiveness of the proposed method is tested on Cosmo-Skymed Spotlight SAR data of maritime targets. Furthermore, the present Doppler Parameter Estimation Algorithm (DPEA) is compared with a well known ISAR technique, namely the Image Contrast Based Technique (ICBT).

Index Terms

ISAR, Doppler Parameters Estimation Algorithm, Image Contrast Based Technique, Doppler Centroid, Doppler Rate.

I. Introduction

SAR imagery is widely used in several applications, spanning from risk monitoring associated with natural and human induced hazards [1] to homeland security and military applications [2]. Classical SAR processing is based on the assumption that the illuminated area is static during the synthetic aperture formation. This allows the SAR system to implement a data focusing, which results in the synthesis of a large virtual array along the platform trajectory, to provide very

high resolution images. When the platform trajectory deviates from its nominal path, motion compensation techniques can be applied to correct the motion errors induced by the platform deviations. Nevertheless, the assumption that the illuminated area does not move during the data acquisition, or better that the movement is stationary on the whole scene, must still hold. In some scenarios, moving targets may be present in an illuminated scene. Such targets, do not satisfy the above mentioned assumption: the mismatch between the target doppler history and the doppler history pertinent to the whole scene used in the reference function induces first of all an azimuth shift, thus providing an incorrect location of the target in the SAR image, and secondly it generates a defocusing of the target (a practical example is shown in figure 1). This is the case of ground vehicles, ships and any other moving targets that may be of interest in some applications. The problem of focusing moving targets in SAR imagery has been addressed in the past and solved in a number of ways. With the advent of very high resolution spaceborne sensors of last generation satellites, namely COSMO/SKYMED and TERRASAR-X, defocusing of moving targets is evident also of SAR images acquired from the space. In [3] it is proposed an algorithm able to detect moving targets and to estimate the correct position within the SAR image (moving target re-location). The evaluation of the target correct position is performed estimating the Doppler shift related to the target motion. This algorithm, however, does not compensate for the phase errors induced by the motion itself. Furthermore, it needs a sequence of SAR images of the same target to estimate its motion parameters.

In [4] [5] it is considered the moving target focusing problem in SAR images, acquired by the SAR system Spotlight: PAMIR. In such papers in order to estimate, with very high accuracy, the motion of the target a tracking system based on the Kalman filter is used. The kalman filter predict the target trajectory exploiting the a-priori knowledge of a road map of the target. Unfortunately, in the real cases, the path followed by the target might be not easily predictable and known a-priori.

Typically, a uniformly accelerated rectilinear motion of targets is assumed [6] [7] [8] [9] to perform the target motion compensation. However, in [10] and [11] more complex motion, involving translational and rotational movements have been considered. In particular, to perform the motion compensation, in [10] Rigling developed a method based on the image-quality optimization that seek to correct the phase history minimizing the entropy. On the other hand, in [11], an algorithm which requires the presence of multiple prominent points in the image of the

target was developed to perform the target motion compensation. Another solution proposed for SAR data refocusing and applied to high resolution data is based on use of the ISAR focusing approach using the image contrast maximization and have been proposed in [13]. Differently from the contributions present in the literature, in this work we propose a novel fast method that is able to achieve effective moving target image focusing that is based on simple target Doppler parameter estimation commonly implemented in classical SAR focusing. Modern spaceborne SAR sensors are equipped with precise GPS and attitude measurement systems that provide accurate estimation of the Doppler parameter used to focus the data with respect to a fixed scene or a scene moving stationary. The SAR literature is however rich of contributions describing autofocusing algorithms tailored to the estimation of Doppler parameters (centroid and rate) and frequently used for focusing data of past generation sensors characterized by inaccurate attitude and orbital measurement systems [16] [17] [18] [19] [20] [21]. Such procedures are able to provide very accurate measurements of the doppler parameter: in focusing of data acquired by modern sensors they are used to refine the information included in the ancillary data to provide higher quality images. Similarly to the literature we approximate the relative distance between a reference point on the target and the sensor by a second order polynomial, the linear and the quadratic terms of the polynomial being related to the Doppler centroid and the Doppler rate, respectively. A way to achieve the estimation of the Doppler centroid is based on image azimuth autocorrelation [17] and on the interference of range looks [18]. The Doppler rate can be estimated by using an iterative procedure that seeks to minimize the mis-registration error between images corresponding to different azimuth looks [19]. Many other approaches are possible, see references in [16] and [22], but the above procedures are rather popular due to their simplicity and effectiveness. The use of such methods to derive a stand-alone algorithm for refocusing moving targets in SAR images provides the main novelty in this work. The rationale of the method is evident from figure 2 and founds on the re-use Doppler parameter estimation tools available in classical SAR focusing to implement the ISAR focusing of moving targets. It should be remarked from now that the presence of multiple moving targets in a SAR scene prevents any algorithm from focusing them simultaneously. For this reason, targets to be focussed should be isolated in advance before processing their data. This can be done directly in the image domain, as shown in [13] [14]. In this paper, we will consider the defocused target's extraction from the SAR image already performed by some other algorithm and will therefore consider only the

problem of refocussing the isolated target. The scenario at hand will be then reduced to that of a moving targets illuminated by a SAR system and processed as a stationary target, which causes an image defocusing to be dealt with. When dealing with imaging of moving targets that are much smaller that the SAR scene it is important to understand that SAR processing is initially used to provide a fine beamforming along the azimuth. Such beamforming, together with the ability to achieve fine range resolution, provides the means to isolate the moving targets from the rest of the SAR scene and concentrate on it, see figure 1, to provide a focussed image. The effectiveness of the proposed technique has been proven by applying it to Cosmo-SkyMed (CSK) SAR data of ships. The proposed method has shown that much more focussed images of the two moving targets can be provided when compared with the original SAR images. Moreover, a direct comparison with the ICBT method, recently proposed in [13] [14], has also been run to provide a substantial comparison to assess the algorithm proposed in this paper. The remainder of this paper is organized as follows. Section II introduces the signal model, which is based on the ISAR concept. Section III concerns one of the Doppler parameter estimation, namely the Doppler centroid, whereas Section IV details the estimation of the second Doppler parameters, namely the Doppler rate. Section V defines the stand-alone algorithm that is able to refocus moving targets in SAR images. Finally, numerical results are shown in Section VI, where CSK data is used to prove the capability of the algorithm to provide well focused images.

II. SIGNAL MODEL

Let refer to the geometry depicted in figure 3 where the sensor is located at $(0, 0, h)$ in the system of coordinates $(\zeta_1, \zeta_2, \zeta_3)$, and let consider the reference system (x_1, x_2, x_3) on the target, which is assumed to move along an arbitrary trajectory. The signal backscattered from the target to the sensor, in the representation of frequency f and slow-time t (sampled at kT_R where T_R is the pulse repetition interval) is given by:

$$S_R(f, t) = rect\left(\frac{t}{T}\right) S_T(f) \int_V \xi(\mathbf{x}) e^{-j4\pi \frac{f}{c} R(\mathbf{x}, kT_R)} d\mathbf{x} \qquad (1)$$

where $\xi(\mathbf{x})$ is the reflectivity function, which represents the backscattering properties of the target, V is the domain where the reflectivity function is defined, c is the speed of light, and $\mathbf{x}$ is the vector that locates a generic scatterer on the target reference system; $R(\mathbf{x}, t)$ is the distance
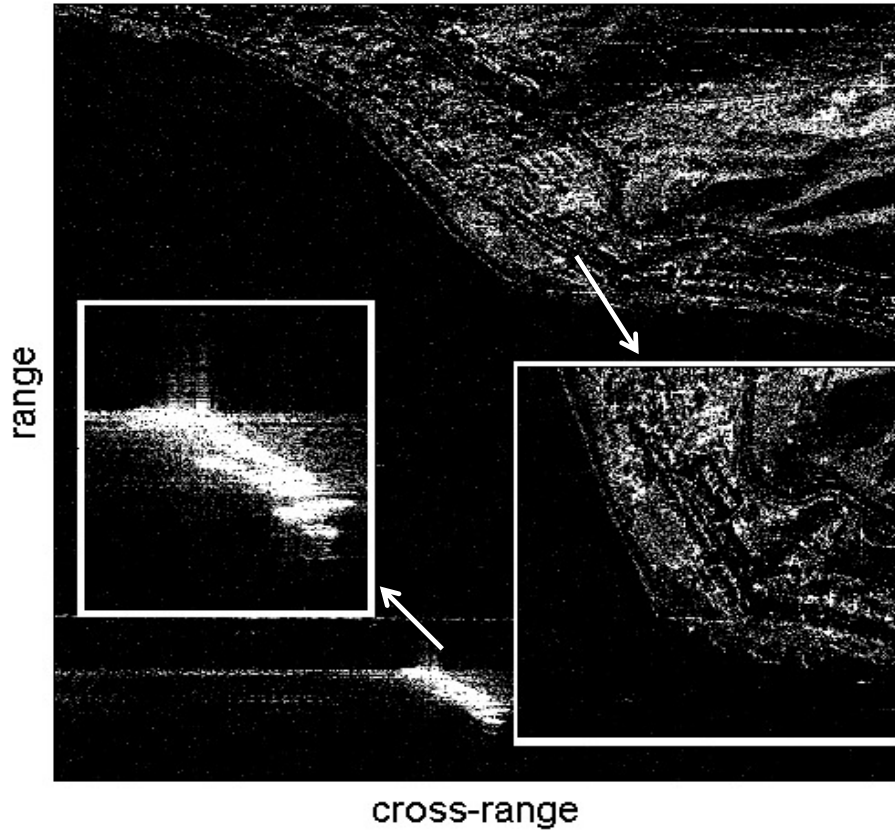
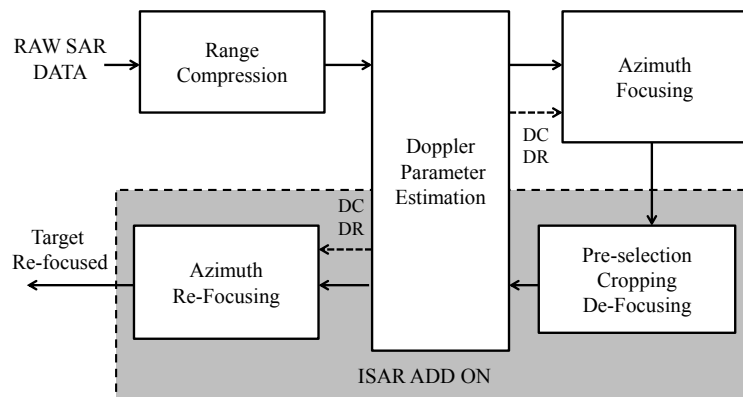Fig. 1: SLC SAR image and relative zoom on the coastal area with the presence of a defocused target.

Fig. 2: ISAR add on Block Diagramm exploiting the SAR Doppler Processing Parameters Estimation Algorithm
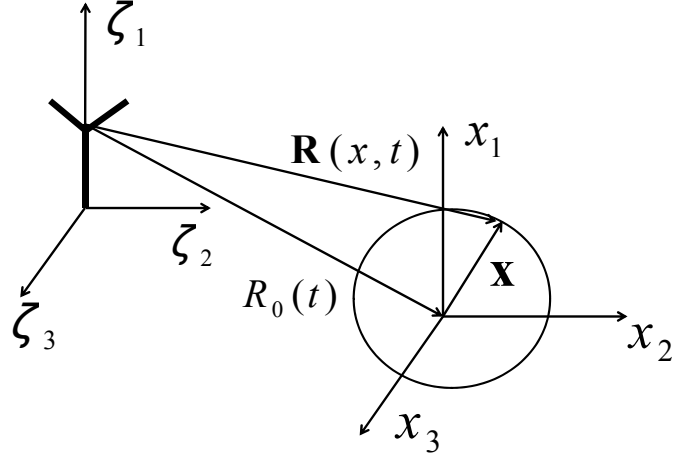
Fig. 3: Reference geometry of the ISAR system with the sensor centred reference system and the reference system moving solidly with the target

between the sensor and the scatterer. We assume that the target observation time is $T = NT_R$ where N is the number of the transmitted pulses.

In a typical ISAR scenario, the target size can be supposed to be significantly smaller then the radar-target distance. Therefore, the iso-range approximation can be applied:

$$R(\mathbf{x}, kT_R) \simeq R_0(t) + \mathbf{x}^T \cdot \mathbf{i}_{LOS}(t) \tag{2}$$

where $\mathbf{i}_{LOS}(t)$ is the line of sight unit vector at time t, and $R_0(t)$ is the modulus of the vector $\mathbf{R}_0(t)$ which locates the position of the focusing point on the target. The received signal in (1) is transformed into the received signal in (3) after applied the iso-range approximation and after splitting the phase into two separated terms, one inside and one outside the integral.

$$S_R(f,t) = W(f,t)e^{-j4\pi\frac{f}{c}R_0(t)} \int_V \xi(\mathbf{x})e^{-j4\pi\frac{f}{c}\mathbf{x}^T \cdot \mathbf{i}_{LOS}(t)}d\mathbf{x} \tag{3}$$

such that:

$$W(f,t) = rect\left(\frac{t}{T}\right) rect\left(\frac{f - f_0}{B}\right) \tag{4}$$

where f_0 is the carrier frequency, B is the transmitted signal bandwidth.

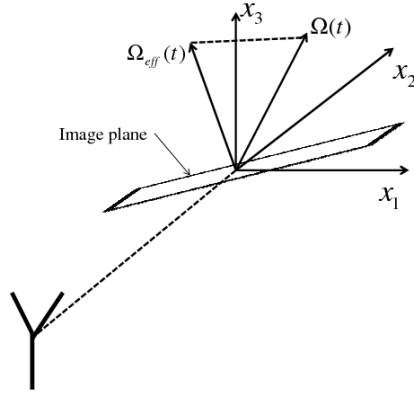The motion of the target is characterized by both translational and angular motion. Both compo-

Fig. 4: Details to of definition of the effective rotation vector and the image plane.

nents produce a target angular motion with respect to a reference system embedded on the radar. Let Ω_{tot} be the total target angular velocity (measured in rad/sec). The effective rotation vector Ω_{eff} can be therefore introduced as the rotational component the produces a target aspect angle variation and therefore a synthetic aperture [14]. In formula, this can be calculated as follows:

$$\Omega_{eff} \triangleq \mathbf{i}_{LOS} \times (\Omega_{tot} \times \mathbf{i}_{LOS}) \tag{5}$$

It is worth pointing out that equation (5) indicates a projection of the total rotation vector onto the plane orthogonal to the Line Of Sight (LOS). The image plane is the plane orthogonal to Ω_{eff}. For the sake of clarity, a pictorial view of the image plane is provided in figure 4. To simplify the following notation, the orientation of the target reference system, which moves solidly with the target, is chosen such that x_3 is orthogonal to the image plane. Accordingly, the image plane is coincident with the plane (x_1, x_2). Referring to the figure 5, the image plane is also the plane where it can be defined the aspect angle $\theta(t)$ which provide the components of the line of sight vector. So the scalar product in (2) can be therefore written as:

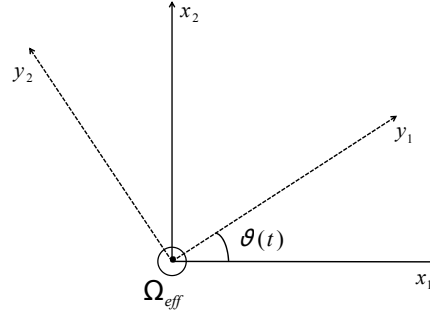$$\mathbf{x}^T \cdot \mathbf{i}_{LOS}(t) = x_1 \sin\theta(t) + x_2 \cos\theta(t) \tag{6}$$

Fig. 5: Definition of the aspect angle $\theta(t)$ respect to the image plane (x_1, x_2).

Accordingly, by defining the following transformation:

$$\Psi : \begin{cases} X_1 = \dfrac{2f}{c}\sin\theta(t) \\ X_2 = \dfrac{2f}{c}\cos\theta(t) \end{cases} \tag{7}$$

the signal in (3) can be expressed as:

$$S_R(f,t) = W(f,t)e^{-j4\pi\frac{f}{c}R_0(t)}\int\int \boldsymbol{\xi}(x_1,x_2)e^{-j2\pi(X_1x_1+X_2x_2)}dx_1dx_2 \tag{8}$$

where $\int \boldsymbol{\xi}(x_1,x_2,x_3)dx_3 = \boldsymbol{\xi}(x_1,x_2)$ is the projection of the reflectivity function on the image plane. Analyzing the terms of the backscattered signal from the target the operations to be performed in order to reconstruct the image of the target can be now described. First of all the motion compensation, which consist of removing the phase term $exp\{-j(4\pi f/c)R_0(t)\}$ owing to the radial motion parameter of the focusing point, should be carried out. After the motion compensation the received signal can be written as:

$$S_R(f,t) = W(f,t)\int\int \boldsymbol{\xi}(x_1,x_2)e^{-j2\pi(X_1x_1+X_2x_2)}dx_1dx_2 \tag{9}$$

In order to form an ISAR image, a 2-IDFT of (9) must be carried out, in the domain defined by (7). In order to implement an efficient 2-IDFT, an FFT algorithm should be used. For aspect angle changes of few degree ($\theta(t) < 5°$) and by considering smooth target's rotation ($\theta(t) = \Omega_{eff}t$), the polar grid in (7) can be approximated with a rectangular grid with evenly spaced samples and therefore an FFT can be applied without introducing significant errors. Such an approach is known in literature as Range-Doppler ISAR processing [14] and [22]. Under such assumptions,

the received signal in (9) can be rewritten as follows:

$$S'_R(f,t) \approx W(f,t) \int \int \boldsymbol{\xi}(y_1,y_2) e^{-j2\pi \frac{2f_0}{c} \frac{\Omega_{eff}}{T} y_1 t} e^{-j2\pi \frac{2f}{c} y_2} dy_1 dy_2. \tag{10}$$

In order to evaluate the system Point Spread Function (PSF) we assume the presence of a single point scatterer located in an arbitrary position (x_1, x_2, x_3). The PSF can be derived by calculating the Fourier Transform of (10). Details of this calculation can be found in [23] and the result is show in (11):

$$I(\tau, f_d) = TB \left| sinc \left[B \left(\tau - \frac{2x_2}{c} \right) \right] \right| \left| sinc \left[T \left(f_d - \frac{2f_0 \Omega_{eff}}{c} x_1 \right) \right] \right| \tag{11}$$

where τ is the round trip delay, f_d is the doppler frequency. The cross-range and range resolution can be calculated as follows [22]:

$$R_{x_1} = \frac{c}{2f_0 \Omega_{eff} T} \quad and \quad R_{x_2} = \frac{c}{2B} \tag{12}$$

When the relative motion between the sensor and the target is regular, the distance $R_0(t)$ can be approximated (around the central time instant $t = 0$) by second order Taylor polynomial:

$$R_0(t) \approx R_0 + \beta t + \gamma t^2 \tag{13}$$

where $\beta = \dot{R}_0(0)$ and $\gamma = \ddot{R}_0(0)/2$. Therefore, in order to perform the motion compensation procedure the estimation of this parameter is fundamental. The estimation of the first term $R_0 = R_0(0)$ can be avoided, as it only causes a constant shift along the range coordinate without defocusing the image [24]. The coefficients β and γ phisically represent the target's radial velocity and acceleration. They are also related to the Frequency Doppler Parameter. Indeed, by differentiating the expression of the phase of the motion compensation term with respect to the slow-time t we obtain the istantaneous Doppler frequency:

$$f_d(t) = f_{DC} + f_{DR} t \tag{14}$$

where f_{DC} is the Doppler Centroid and f_{DR} the Doppler Rate, whose binding to the coefficients

β and γ are:

$$\begin{cases} f_{DC} = & \dfrac{2f}{c}\beta \\[2mm] f_{DR} = & \dfrac{4f}{c}\gamma \end{cases} \tag{15}$$

the motion coefficients, namely β and γ, can be therefore calculated by estimating the Doppler parameters (f_{DC} and f_{DR}).

III. DOPPLER CENTROID ESTIMATION

In the previous section, we showed the important relationship between the motion parameters and the signal Doppler parameters. In this section, we will discuss how to estimate the Doppler Centroid by using an algorithm implemented by Madsen [17] which is typically used in standard SAR image focusing. In particular we will describe how this algorithm is modified to adapt to an ISAR configuration. The Doppler centroid plays an important role in the cross-range processing. In fact, this parameter is directly related to the target's radial velocity and also represents the average Doppler shift, which affects the backscattered signal. With reference to (8), let define the following function:

$$S(f,t) \triangleq W(f,t)e^{-j2\pi\frac{2f}{c}\gamma t^2} \int \int \boldsymbol{\xi}(x_1,x_2)e^{-j2\pi(X_1x_1+X_2x_2)}dx_1dx_2 \tag{16}$$

To simplify the notation we will consider only the dependence on t and will temporally neglect the depence on f. Therefore, the received signal can be written as:

$$S'_R(t) = S(t)e^{-j2\pi\frac{2f_0}{c}\beta t} \tag{17}$$

where $\frac{2f_0}{c}\beta$ is the Doppler Centroid f_{DC}. Let us now consider the function $P(f_d)$ defined as the power doppler spectrum associated to the signal $S(t)$. Therefore the power doppler spectrum of $S'_R(t)$, can be written as:

$$P_s(f_d) = P(f_d - f_{DC}) \tag{18}$$

The autocorrelation function $R_s(\eta)$ can then be calculated as the IFT of $P_s(f_d)$, as follow:

$$R_s(\eta) = FT^{-1}[P_s(f_d)] = R(\eta)e^{j2\pi\eta f_{DC}} \tag{19}$$

with

$$R(\eta) = FT^{-1}[P(f_d)] \tag{20}$$

As the signal $S(t)$ is sampled in the time domain, we must substitute $\eta = kT_R \quad k = 0, 1, \ldots, N-1$ in 19, as follows:

$$R_s(k) = R(k)e^{j2\pi kT_R f_{DC}} \tag{21}$$

So, in the time domain, measuring the phase of the correlation coefficient is possible to estimate the Doppler centroid, as:

$$\hat{f}_{DC} = \frac{1}{2\pi kT_R} arg\{R_s(k)\} \tag{22}$$

Because the sampling step T_R may be not small enough, the Doppler estimation may be affected by an aliasing error. For this reason, the centroid can be considered as composed of two parts: an integer number, namely the Doppler Ambiguity, and the fractional part, which can be interpreted as the wrapped doppler centroid. In formula, this can be expressed as follow:

$$f_{DC}' = \hat{f}_{DC} + M \cdot PRF \tag{23}$$

Where f_{DC}' is the unwrapped Doppler Centroid, $\hat{f}_{DC}$ is the estimated wrapped Doppler Centroid. The estimator presented in (22) is able to provide the wrapped doppler centroid. In order to correctly estimate the Doppler centroid, also the ambiguity number M must be estimated. In this work, such number is estimated by using the Multi-Look Beat Frequency (MLBF) algorithm, which was developed by Cumming for the SAR system [18].

With reference to the formula (8) let define the two range compressed looks of a single point target that are shifted by a frequency Δf:

$$\mathfrak{L}_1(f,t) = rect\left(\frac{t}{T}\right) rect\left(\frac{f - f_0 - \frac{\Delta f}{2}}{B}\right) \exp{-j4\pi\left(\frac{f_0 - \frac{\Delta f}{2}}{c}\right)} R(t) \tag{24}$$

$$\mathfrak{L}_2(f,t) = rect\left(\frac{t}{T}\right) rect\left(\frac{f - f_0 + \frac{\Delta f}{2}}{B}\right) \exp{-j4\pi\left(\frac{f_0 + \frac{\Delta f}{2}}{c}\right)} R(t) \tag{25}$$

The MLBF algorithm calculates the beating product between two range looks the result is as follows and the details can be found in Appendix A:

$$f_b(t) = \frac{\Delta f}{f_0} \left(f'_{DC} + f_{DR}t \right) \tag{26}$$

Assuming that the slow-time signal envelope is symmetric with respect to the doppler centroid and that the doppler bandwidth is confined in a narrow range, a relation between the beat frequency f_b and the unwrapped doppler centroid can be obtained averaging the envelope in the slow-time domain, as follows

$$f_b = f'_{DC} \frac{\Delta f}{f_0} \tag{27}$$

The frequency of the beat signal is calculated by transforming the beating signal in the Doppler domain and by evaluating the position of the maximum value of its mean power (average along the range coordinate). The averaging operation makes this estimation robust with respect to the presence of clutter in the real data. By estimating the beating frequency and by inverting the formula (27) we can obtain the unwrapped centroid. However, rather than to calculate the centroid with the MLBF algorithm (due to the presence of noise and the contribution of extended targets that could cause some estimation errors), in this paper, the MLBF is performed only to calculate the Doppler Ambiguity. The Doppler Centroid fractional part is instead estimated by using Madsen's algorithm. The unwrapped Doppler centroid is then obtained by using (23).

IV. DOPPLER RATE ESTIMATION

The algorithm for estimating the Doppler rate originates from an algorithm developed for SAR image auto-focus by Curlander at al. [19]. The algorithm is able to correct the inaccuracies on the knowledge of motion parameters, which, in the SAR case, are tipically known a priori. In fact, the SAR Doppler rate can be easily calculated by knowing the sensor parameters $f_{DR}^{(SAR)} = 2v_r^2/\lambda r_0$ where v_r is the radial velocity of the sensor, λ is the radar wavelength and r_0 is the reference distance between the radar and the scene centre. Often, however, the measured parameters are affected by errors that lead to an inaccurate estimation of the Doppler Rate. For this reason, algorithms have been developed in the literature to correct the parameter estimates, and achieve a better motion compensation. The proposed algorithm uses a sub-aperture correlation method [20]. This method relies on the well known relationship between slow-time coordinates and the
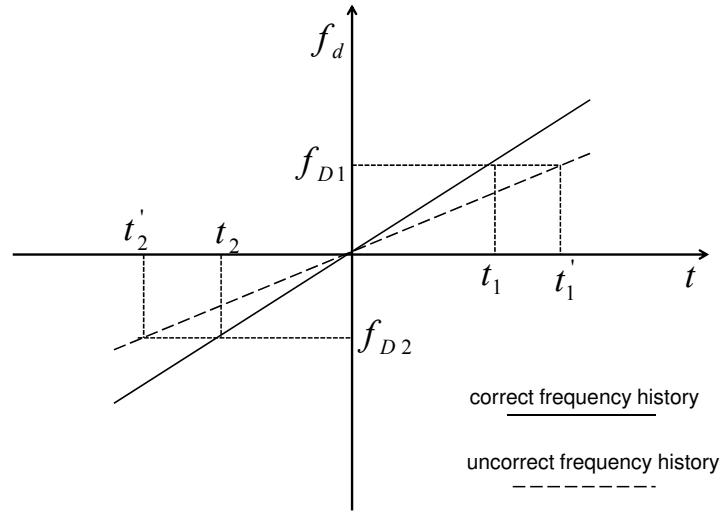
Fig. 6: Slow-TIme and Doppler Frequency relation.

Doppler frequency:

$$f_d = f_{DR}t \tag{28}$$

In particular such an algorithm considers two sub-apertures that are generating by filtering the received signal in the Doppler domain. Specifically, two Doppler sub-bands centered around two frequencies, namely f_{D1} and f_{D2}, are defined where the signal is filtered. Once the two sub-apertures are obtained after filtering the original signal, the two SAR images are formed, one per sub-aperture. If the nominal value of the Doppler rate (f'_{DR}) is used to compensate the platform motion, a SAR image will be produced that shows a time shift with respect to its correct position. Such time shift can be calculated as follows:

$$\epsilon_k = t'_k - t_k = \frac{f_{Dk}}{f'_{DR}} - \frac{f_{Dk}}{f_{DR}}, \quad k = 1, 2 \tag{29}$$

where f_{DR} is the correct value of the Doppler rate. A de-focusing effect would also be notice if $t'_k - t_k \neq 0$ and it would be more pronounced if $t'_k - t_k$ increases. The two SAR images would show a time shift difference:

$$\Delta t = \epsilon_1 - \epsilon_2 \tag{30}$$

when the incorrect Doppler rate is used to compensate the platform motion. Whereas, if $f'_{DR} = f_{DR}$, no time shift difference would be present. In fact, a relationship between the time shift difference Δt and the Doppler rate f_{DR} can be written as follow:

$$\Delta t = (f_{D2} - f_{D1}) \left(\frac{1}{f'_{DR}} - \frac{1}{f_{DR}} \right) \tag{31}$$

An estimation of f_{DR} can be obtained by inverting (31). It should be pointed out that f_{DR} can be estimated by iterating this process, as consecutive iterations improve the estimation of Δt, which is typically attained by cross-correlating the two sub-apertures SAR images and by finding its peak.

In the ISAR context, though, the two sub-apertures images are defined in the Range-Doppler domain (see (11)), which changes some of the aspects of this method. In order to modify this method to apply to the ISAR case, we have recalculated the sub-apertures ISAR image mathematically expressions. Details of such calculation are given in Appendix B. The direct result of the cross-correlation is given in (32):

$$R_{\Gamma_{l1},\Gamma_{l2}}(\nu) = |\Gamma_{l1}(f_d)|^2 \otimes |\Gamma_{l2}(-f_d)|^2 (\nu) =$$

$$FT^{-1} \left\{ \Lambda \left(\frac{t}{T/2} \right) e^{-j2\pi\alpha\frac{T}{4}} \Lambda^* \left(\frac{t}{T/2} \right) e^{-j2\pi\alpha\frac{T}{4}} \right\} =$$

$$= FT^{-1} \left\{ \left| \Lambda \left(\frac{t}{T/2} \right) \right|^2 e^{-j2\pi\alpha\frac{T}{2}} \right\} = A \left(\frac{\nu - \alpha T/2}{2/T} \right) \tag{32}$$

where ν is the doppler lag and α is the Doppler rate error, defined as follow:

$$\alpha = f_{DR} - f'_{DR} \tag{33}$$

Γ is the sub-aperture Doppler profile defined in the Appendix B , Λ is the triangular function defined as follows:

$$\Lambda \left(\frac{t}{T/2} \right) = rect \left(\frac{t}{T/2} \right) (1 - |t|) \tag{34}$$

and A is the Inverse Fourier Transform of the triangular function square modulus. It is worth noting that the function A can also be obtained by convolving two $sinc$ functions. In the case of a very bright scatterer, its PSF can be considered equivalent to a $sinc$ function and therefore, as result, the cross-correlation would produce a concentrated peak at the position $\alpha T/2$. In this

case, the result of the search of the cross-correlation peak would return such position:

$$\widehat{\nu}_{max} = argmax_\nu \left\{ R_{\Gamma_{l1}, \Gamma_{l2}}(\nu) \right\} = \alpha \frac{T}{2} \tag{35}$$

Which would lead to an estimation of the Doppler rate error, as follow:

$$\widehat{\alpha} = \frac{2}{T} \widehat{\nu}_{max} \tag{36}$$

The subsequent estimation of the Doppler rate would be obtained as follows:

$$\widehat{f}_{DR} = f'_{DR} + \widehat{\alpha} \tag{37}$$

As already mentioned, this procedure can be iterated by updating f'_{DR} with $\widehat{f}_{DR}$. The iteration may stop when the difference between two consecutive iteration is small than a pre-set threshold. In the ISAR case, it is also important to obtain an initial guess for f'_{DR}. In this paper, we estimate such initial guess by exploiting the relationship between the Doppler bandwidth and the observation time:

$$B_d = f'_{DR} T \tag{38}$$

The Doppler Bandwidth is here considered as the support of the cross-range power spectral density. This can be measured by using one of the conventional definitions (e.g. $-3dB$ Doppler bandwidth or 99% of the energy).

V. DOPPLER PARAMETERS ESTIMATION ALGORITHM FOR SAR RE-FOCUSING

In sections III and IV we have introduced the methods for estimating the Doppler Centroid and Doppler Rate, respectively. However, we will detail in this section how these methods are joined together into an algorithm that will able to refocus non-cooperative target in Single Look Complex SAR images. In fact, when the SAR image is focused, the SAR processor considers only the relative motion between the platform that carries the sensor and one single point of the illuminated area, which is taken as a reference point of a static observation scene. Therefore, targets that are in motion during the Coherent Processing Interval (CPI), appear de-focused in the SAR image. This phenomenon becomes more evident when the CPI increases. The goal of the proposed algorithm is to estimate the target's Doppler Parameters (Centroid and Doppler Rate) using a defocused SLC SAR image of it as input data. The refocus algorithm is designed
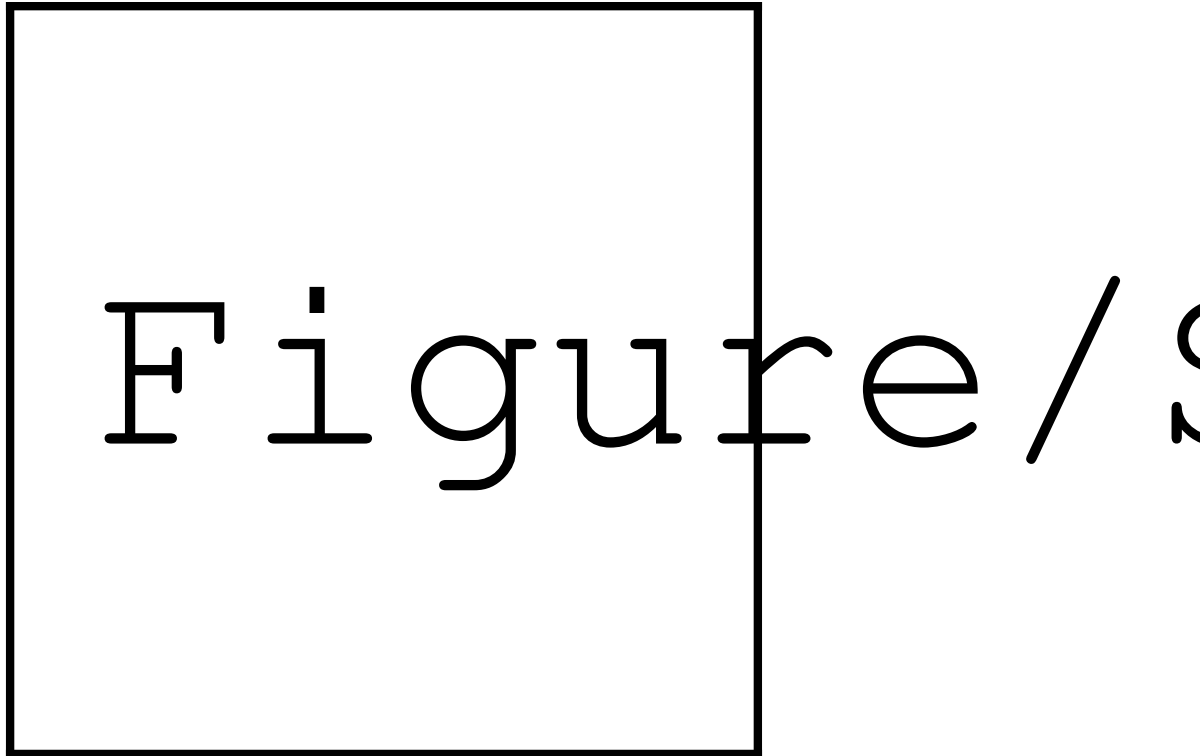
Fig. 7: Block diagram of Doppler Parameters estimation for the re-focusing non-cooperative targets. The dashed lines connections indicate that the estimated Doppler rate is updated at each iteration.

to be applied to both StripMap and Spotlight SAR modes. A block diagram of the proposed algorithm is shown in figure 7.

The proposed algorithm takes a crop of the de-focused target from the SLC SAR image as input and then estimates the Doppler centroid by using the algorithm described in section III. The Doppler centroid estimation is performed in two steps. The first step makes use of the algorithm developed by Madsen, which exploits the Fourier Transform relationship between the power spectrum of the signal along the slow-time and its autocorrelation function. The Doppler centroid is estimated as indicated in (22). A common practices (see [21]) the lag value is set to $k = 1$. This allows the autocorrelation function to be evaluated near the peak, therefore ensuring sufficiently high Signal to Noise Ratio (SNR).

If the slow-time sampling rate is below Nyquist, the Doppler centroid estimation may produce an estimate that is a wrapped version of the actual value. For this reason, a second step is performed. The second step evaluates the doppler ambiguity by applying the MLBF algorithm:

a check is carried out that aims at determining if the estimate Doppler centroid is the correct one or if it is wrapped. In the latter case, the Doppler ambiguity factor (M) is determined firstly and the Doppler centroid is re-estimated by using (23).

After estimating the Doppler centroid, the refocus algorithm proceeds with the Doppler Rate estimation. As previously explained, the Doppler rate estimation is performed by using an iterative algorithm that seeks to minimize the estimation error, starting from the initial knowledge of a nominal Doppler Rate. Such nominal rate is a parameter that is set a priori and, in this case, is the Doppler Rate that was used by the SAR processor to carry out the motion compensation procedure to form the original SLC SAR image $f_{DR}^{(SAR)}$. At first, the algorithm filters the two sub-apertures that have to be cross-correlated. After doing that, both SAR images obtained with the two sub-apertures are de-focussed by the following deramping factor:

$$d(f, t^{'}) = e^{+j2\pi \frac{2f}{c} \widetilde{R}_0(t^{'})} \tag{39}$$

where the distance term is:

$$\widetilde{R}_0(t^{'}) = f_{DC}^{(SAR)} t^{'} + f_{DR}^{(SAR)} t^{'2}. \tag{40}$$

and where $t^{'}$ is the is a scaled version of the slow-time. This de-focusing procedure is performed in order to reconstruct the signal back-scattered from a classical ISAR point of view and then the data is processed according to the proposed estimation process.

Subsequently, the two sub-apertures are refocused with the distance term:

$$\widehat{R}_0(t^{'}) = \widehat{f}_{DC} t^{'} + \widehat{f}_{DR} t^{'2}. \tag{41}$$

It should be pointed out that the term $\widehat{R}_0(t^{'})$ does not remain constant because the Doppler Rate $\widehat{f}_{DR}$ is updated at each iteration. Finally, the two sub-apertures are cross-correlated to measure the mis-registration parameter Δt defined in (28), which allows determining if the estimated doppler rate, namely $\widehat{f}_{DR}$ is equal or not to the actual Doppler Rate. Consequently, the Doppler Rate is updated again. The same steps are repeated as long as the two sub-apertures are mis-registered ($\Delta t \neq 0$).

The scheme described above is the most general scheme for re-focusing of the non-cooperative

targets in the focused SAR images. The algorithm can be further improved especially with respect to the computational load and time complexity point of view. In particular, in the Stripmap case, the de-focusing procedure can be performed before the two sub-apertures filtering steps and performed only once. On the other hand, in the Spotlight case, the sub-apertures filtering cannot be performed after the de-focusing due to the well known spectral aliasing [25]. Moreover, if a good pre-estimate of the Doppler Rate is available, further improvement in term of computational load can be achieved because the filtering process can be performed only at the first iteration. More specifically as far as the sub-aperture filtering blocks in figure 7 are concerned, it can be operated a substitution of $\widehat{f}_{DR}$ with $f_{DR}^{(SAR)}$. This substitution leads to a scheme in which the dash line in figure 7 corresponding to the iteration can be limited to the focusing procedure block, without reaching the sub-aperture filtering block diagram.

VI. NUMERICAL RESULTS

The Doppler Parameter Estimation Algorithm (DPEA) described in the previous section has been tested with SAR data provided by Italian Space Agency (ASI) under a Cosmo-SkyMed (CSK) AO Project [26]. Specifically, SLC SAR images of moving maritime targets have been used. In order to validate the proposed technique on Spotlight SAR images, we have proposed two case studies. Some specification of the Spotlight SAR data are summarized in Table I. The scenario selected is such that the observation time is short enough to guarantee that the target's effective rotation vector is constant. The results obtained by using the proposed estimation algorithm are compared to the results obtained by using the Image Contrast Based Technique (ICBT) [24]. The latter has been chosen as a term of reference as it is a well consolidated and effective algorithm for refocusing moving targets in SAR images [12] and [13]. The comparison analysis between the two different algorithms has been carried out by considering:

- image visual quality;
- image contrast;
- entropy of the image intensity;
- peak value of the image intensity;
- computational load.

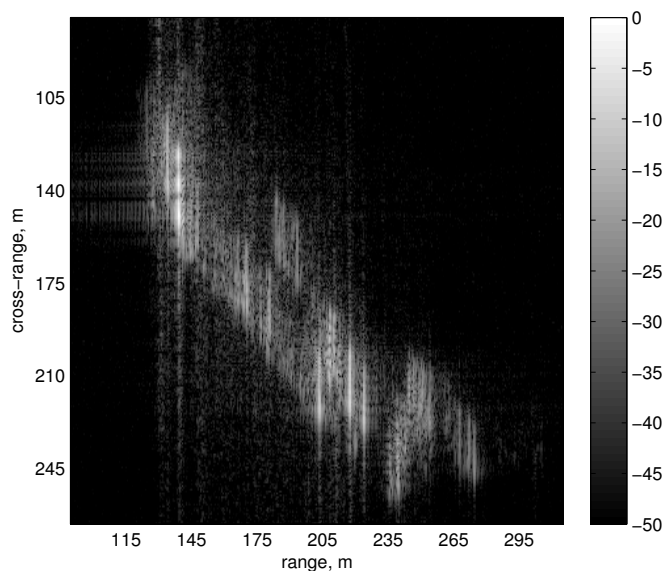| Parameters	SAR Spotlight Image 1	SAR Spotlight Image 2
PRF, kHz	9.809	9.712
B, MHz	277.510	198.410
T_{obs},s	2.080	2.588
Polarisation	HH	HH
Look	right	right
Direction	descending	ascending

TABLE I: SAR Image Specification

Fig. 8: First unfocused ship cropped from the SLC image of CSK in Spotlight mode.

A. First Case Study: Image 1

We have considered the problem of refocusing a SLC SAR image of a moving ship. The image was collected by CSK in spotlight mode. As evident from the figure 8 the image has a greater de-focusing effect. This phenomenon may be due to the fact that the SAR Spotlight mode requires a longer integration time and therefore the target's motions become more evident in the formation of the synthetic aperture. It should not be excluded though that the target may have had faster and more complicated motions. The images obtained using the two refocusing techniques are shown in figures 9 and 10 respectively. From a visual inspection, both images seem to have achieved an optimal result in terms of image refocus. In fact, the scattering centers representative of strong scattering mechanisms are well mapped into single points in the refocussed image.
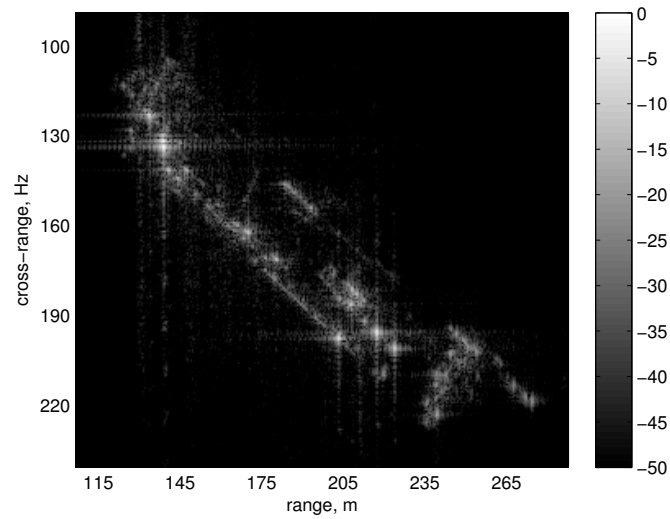
Fig. 9: First focused ship with Doppler Parameters Estimation algorithm.
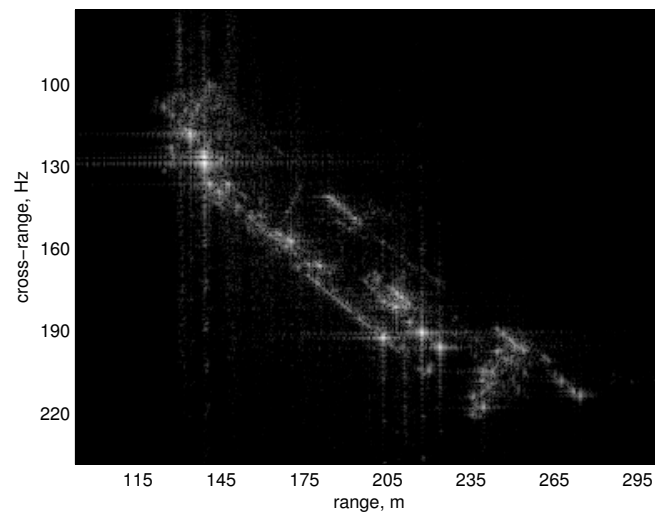
Fig. 10: First focused ship with Image Contrast Based Technique.

Also, the contours of the ship are much more delineated than in the original image. The results in terms of image contrast, entropy and peak reflect the visual inspection results, as shown in table II. The DPEA achieves, albeit slightly, a lower entropy and same value of contrast. Furthermore, the DPEA obtains a higher image peak. This is reflected by the higher localization and lower side-lobe-level (SSL) of some scatterers, which can be noticed by comparing figures 9 and 10.

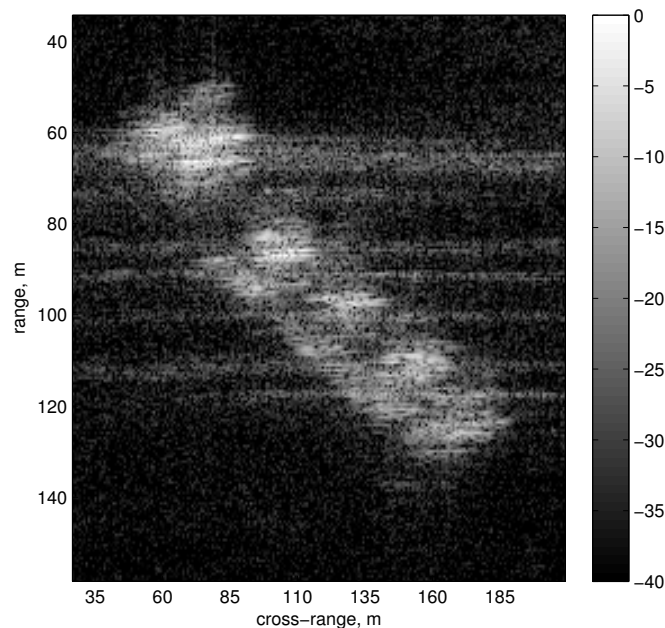| Parameters	SAR processing	DPEA	ICBT
Centroid, Hz	$7.462 \cdot 10^6$	$1.320 \cdot 10^4$	$7.462 \cdot 10^6$
Doppler Rate, Hz/s	$3.098 \cdot 10^3$	$3.105 \cdot 10^3$	$3.593 \cdot 10^4$
Constrast	3.641	4.329	4.329
Entropy	7.774	6.350	6.359
Peak	$3.757 \cdot 10^3$	$1.015 \cdot 10^4$	$8.866 \cdot 10^3$
Computational load, s		1.934	2.980

TABLE II: Comparison Parameters for Image 1

Fig. 11: Second unfocused ship cropped from the SLC image of CSK in spotlight mode.

B. Second Case Study: Image 2

As second case study, we considered the problem of re-focusing a moving ship in a SLC SAR image, which appears de-focused in both range and azimuth directions (see figure 11). If compared to the first case, the second image shows a greater de-focusing effect. It should not be excluded though that the target may have had faster and more complicated motions than in the first case study as the result of a higher sea state or because it was undergoing some maneuvers during the observation time.

From a visual point of view (see figure 12), the image obtained by using the DPEA seems
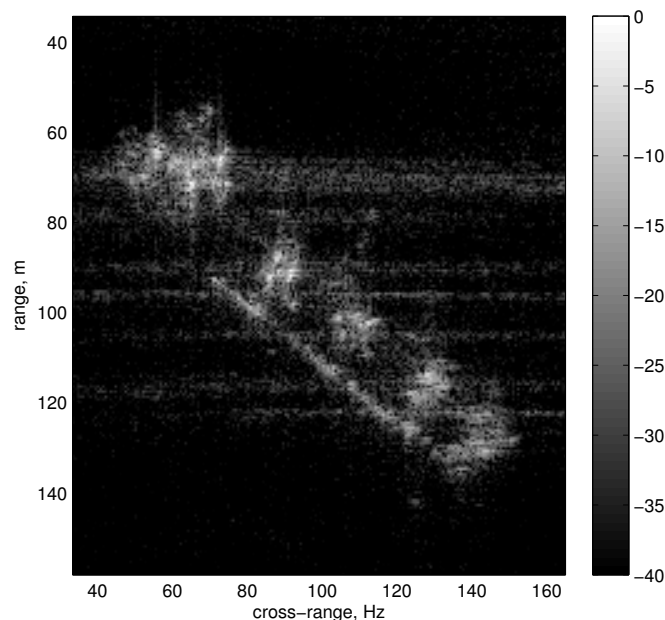
Fig. 12: Second focused ship with Doppler Parameters Estimation Algorithm.

Parameters	*SAR processing*	*DPEA*	*ICBT*
Centroid, Hz	806.970	464.305	806.915
Doppler Rate, Hz/s	$3.895 \cdot 10^3$	$3.892 \cdot 10^3$	$3.884 \cdot 10^3$
Constrast	1.871	2.014	2.020
Entropy	8.667	8.070	8.063
Peak	$1.281 \cdot 10^3$	$2.646 \cdot 10^3$	$2.492 \cdot 10^3$
Computational load, s		1.213	1.92

TABLE III: Comparison Parameters for Image 2

very well focused, as highlighted by the vessel contours. In addition, the DPEA reduces also the spread along the azimuth coordinate, as shown in the original SLC SAR image. Indeed, the vessel appears with a thinner outline. Furthermore, the image focus achieved by the DPEA has enhanced the signal-to-clutter ratio (SCR).

On the other hand, the ICBT (see figure 13) obtains very similar results to those obtained with the DPEA. In fact, the images look almost indistinguishable. When looking at the results shown in table III, the ICBT shows, although for few decimal values, a lower value of the image contrast, indeed, the contrast is the parameter that the ICBT aims to maximize. As far as the entropy is concerned [27], again, the DPEA seems to obtain, although for a few of decimal digits,
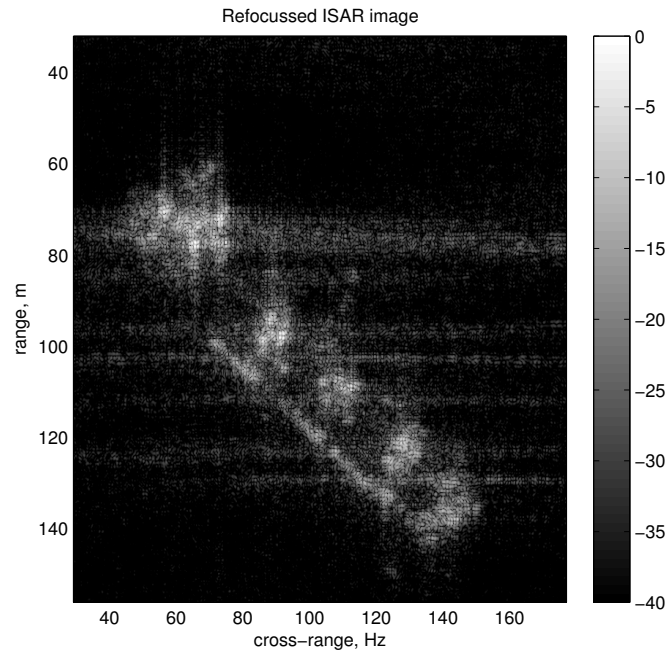
Fig. 13: Second focused ship with Image Contrast Based Technique.

a lower entropy. In terms of image peak, the DPEA produces the highest value, indicating its ability to well focus with respect one point of the target. Considering such a point as a reference point on the target, this indicates the DPEA's effectiveness to track the Doppler centroid and Doppler rate (radial velocity and acceleration) of the target. This results prove the effectiveness of the DPEA.

VII. CONCLUSION

In this paper an ISAR autofocusing algorithm based on Doppler parameter estimation has been proposed. The algorithm is based on the re-use of Doppler parameter estimation tools available in classical SAR focusing and adapted to perform the ISAR focusing of moving targets. The algorithm assumes that the distance of a reference point on the target from the radar can be approximated by a second order polynomial. The algorithm firstly estimates the Doppler centroid in two steps: (1) estimates the fractional part of the Doppler Centroid by evaluating the phase of the correlation coefficient of the received signal envelope along the cross-range, (2) estimates the Doppler ambiguity by using the Multi-Look Beat Frequency MLBF algorithm and by measuring the beating frequency between two cross-range envelopes of the backscattered signal. Finally,

the algorithm estimates the Doppler rate by using an iterative procedure that minimizes the mis-registration error between two cross-range sub-apertures. The effectiveness of the proposed algorithm has been proven by testing it with a real dataset and by comparing the results with a well-established autofocus technique. From a visual point of view and in terms of image contrast and entropy, the DPEA has shown very good results, which are comparable with those obtained by the ICBT. Furthermore, the DPEA seems to produce consistently a higher image peak value and it runs at slightly lower computational cost, making it a strong candidate for a real-time ISAR image autofocus technique.

APPENDIX A

The relationship between the Doppler Centroid and the beating frequency is derived in the appendix. To do that, we will consider two range compressed looks defined in (42) and (43), in particular, fixing the two frequencies $f_1 = f_0 - \Delta f/2$ and $f_2 = f_0 + \Delta f/2$ the range envelopes can be approximated as follow:

$$\mathfrak{L}_1(t) = rect\left(\frac{t}{T}\right) \exp -j4\pi \left(\frac{f_0 - \frac{\Delta f}{2}}{c}\right) R(t) \tag{42}$$

$$\mathfrak{L}_2(f,t) = rect\left(\frac{t}{T}\right) \exp -j4\pi \left(\frac{f_0 + \frac{\Delta f}{2}}{c}\right) R(t) \tag{43}$$

If we consider the phase terms (42) and (43) and the second order polynomial approximation of $R_0(t)$, we obtain:

$$\Phi_1(t) = 4\pi \left(\frac{f_0 - \frac{\Delta f}{2}}{c}\right) \left(R_0 + \beta t + \gamma t^2\right) \tag{44}$$

$$\Phi_2(t) = 4\pi \left(\frac{f_0 + \frac{\Delta f}{2}}{c}\right) \left(R_0 + \beta t + \gamma t^2\right) \tag{45}$$

The beat product between the two range compressed looks becomes then equal to:

$$S_b(t) = \mathfrak{L}_1(t)\mathfrak{L}_2^*(t) = \left|rect\left(\frac{t}{T}\right)\right|^2 e^{+j(\Phi_2(t)-\Phi_1(t))} \tag{46}$$

The beating frequency can then be calculated by differentiating the phase of the signal represented in (46), as follow:

$$
\begin{aligned}
f_b(t) = \frac{1}{2\pi}\frac{\partial}{\partial t}\angle S_b(t) &= \\
2\frac{\Delta f}{c}\left(\beta + 2\gamma t\right) &= \\
\frac{\Delta f}{f_0}\left(2\frac{\beta}{\lambda} + 4\frac{\gamma}{\lambda}t\right) &= \\
\frac{\Delta f}{f_0}\left(f_{DC}' + f_{DR}t\right) &
\end{aligned}
\tag{47}
$$

where $\angle S_b(t)$ is the phase term of (46).

APPENDIX B

The cross-correlation function result in (32) is derived in this appendix. Let the signal in (48) represent the range compressed profile after the radial motion compensation:

$$
S_R''(f,t) = W(f,t)e^{-j2\pi\frac{2f}{c}(R_0+\beta t+\gamma t^2)}e^{-j2\pi\frac{2f}{c}(\widehat{\beta}t+\widehat{\gamma}t^2)}\int\int \boldsymbol{\xi}(y_1,y_2)e^{-j2\pi(x_1\sin\theta(t)+x_2\cos\theta(t))}dx_1 dx_2
\tag{48}
$$

We will now consider the following assumption:

- $\widehat{\beta} = \beta$

- the target is composed of a single scatterer $\xi(x_1, x2) = \sigma_0\delta(x_1, x2))$.

- The constant term R_0 is neglected (it only causes a range shift in the ISAR image).

The signal in (48) can be approximated as follows:

$$
S_R''(f,t) \approx \sigma_0 W(f,t)e^{-j2\pi\frac{2f}{c}\Delta\gamma t^2}
\tag{49}
$$

where $\Delta\gamma = \gamma - \widehat{\gamma}$ is the acceleration estimation error. If we also assume that the range migration due to the residual quadratic term $\Delta\gamma$ is negligible, the frequency range f can replace by the carrier frequency f_0 as follows:

$$
S_R''(f = f_0, t) = S_R''(t) = \sigma_0 W(t)e^{-j2\pi\frac{2f_0}{c}\Delta\gamma t^2}
\tag{50}
$$

It should be noted that by posing $f = f_0$, we neglect the signal dependence on the frequency variable. We now create two sub-apertures by posing $t_1 = T/4$ and $t_2 = -T/4$ and be defining

two new signals:

$$S_{l1}(t) = \sigma_0 rect\left(\frac{t - T/4}{T/2}\right) e^{-j2\pi\frac{2}{\lambda}\Delta\gamma t^2} \tag{51}$$

$$S_{l2}(t) = \sigma_0 rect\left(\frac{t + T/4}{T/2}\right) e^{-j2\pi\frac{2}{\lambda}\Delta\gamma t^2} \tag{52}$$

It should be remarked that $f_{DR} - f'_{DR} = \frac{2}{\lambda}\Delta\gamma$ represents the residual Doppler Rate. For the sake of convinience we will rename $\alpha = \frac{2}{\lambda}\Delta\gamma$. Moreover, being $\alpha T \ll 1$, the expression in (51) (52) can be approximated by their first order polynomial around the points t_1 and t_2, as follows:

$$S_{l1}(t) \approx \sigma_0 rect\left(\frac{t - T/4}{T/2}\right) e^{-j2\pi\alpha\frac{T}{4}t} \tag{53}$$

$$S_{l2}(t) \approx \sigma_0 rect\left(\frac{t + T/4}{T/2}\right) e^{+j2\pi\alpha\frac{T}{4}t} \tag{54}$$

The two Doppler profile can be obtained by FT of (53) and (54). The results can be shown below:

$$\Gamma_{l1}(f_d) = \frac{T}{2}\sigma_0 sinc\left(\frac{f_d - \alpha T/4}{2/T}\right) e^{-j2\pi f_d\frac{T}{4}} \tag{55}$$

$$\Gamma_{l2}(f_d) = \frac{T}{2}\sigma_0 sinc\left(\frac{f_d + \alpha T/4}{2/T}\right) e^{+j2\pi f_d\frac{T}{4}} \tag{56}$$

REFERENCES

[1] D. Massonnet, K. Feigl, M. Rossi, and F. Adragna, "*Radar interferometric mapping of deformation in the year after the Landers earthquake*", *Nature*, pp. 227-230, May 1994.

[2] M. Di Lazzaro, G. Angino, M. Piemontese, A. Capuzi, and R. Leonardi, "*COSMO-SkyMed: The Dual-Use Component of a Geospatial System for Environment and Security*", *IE Aerospace Conference.*, pp. 1 - 10, 2008.

[3] M. Kirscht, " *Detection and imaging of arbitrarily moving targets with single channel SAR*", *IET Radar Sonar Navig.*, Vol. 26, No. 4, pp. 7-11, Apr 2003.

[4] P. Berens, U. Gebhardt, and J. Holzner, "*ISAR imaging of ground moving vehicles using PAMIR data*", *Radar Conference - Surveillance for a Safer World, 2009. RADAR. International*, 2009.

[5] P. Berens, and U. Gebhardt, "*ISAR imaging of ground moving vehicles using large isatntaneous Bandwidth*", *Synthetic Aperture Radar, 2012. EUSAR. 9th European Conference on* , pp. 119-122, 2012.

[6] R.P. Perry, R.C. DiPietro, and R.L. Fante, "*SAR imaging of moving targets*", *IEEE Trans. on Aerospace and Electronic System*, Vol. 35, No. 1, pp. 188-200, Jan. 1999.

[7] S. Zhu, G. Liao, Y. Qu, Z. Zhou, and X. Liu, " *Ground moving targets imaging algorithm for synthetic aperture radar*", *IEEE Trans. on Geoscience and Remote Sensing*, Vol. 49, No. 1, pp. 462-477, Jan. 2011.

[8] F. Zhou, R. Wu, M. Xing, and Z. Bao, " *Approach for single channel SAR ground moving target imaging and motion parameter estimation*", *IET Radar Sonar Navig.*, Vol. 1, No. 1, pp. 125-128, Jan. 2007.

[9] I. Djurovic, T. Thayaparan, and L. Stankovic, " *SAR imaging of moving targets using polynomial fourier transform*", *IET Signal process*, Vol. 2, No. 3, pp. 237-246, March 2008.

[10] B. D. Rigling, " *Image-Quality Focusing of Rotating Targets*", *IEEE Geosci. Remote Sens. Letters*, Vol. 5, No. 4, pp. 750-754, Oct. 2008.

[11] S. Werness, W. Carrara, L. Joyce, and D. Franczak, " *Moving target imaging algorithm for SAR data*", *IEEE Trans. on Aerospace and Electronic System*, Vol. 26, No. 1, pp. 57-67, Jan. 1990.

[12] M. Martorella et all, " *An ISAR Technique for Refocusing Moving Targets in SAR Images*", *Signal and Image Processing for Remote Sensing*, 2nd Edition, CRC Press, Feb. 2012.

[13] M. Martorella, E. Giusti, F. Berizzi, A. Bacci, and E. Dalle Mese, " *ISAR Based Technique for Refocusing Non-Cooperative Targets in SAR Images*", *IET Radar, Sonar and Navig.*, Vol. 6, No. 5, pp. 332-340, May 2012.

[14] T. Cooke, M. Martorella, B. Haywood, and D. Gibbins " *Use of 3D ship scatterer models from ISAR image sequences for target recognition* ", *Elsevier DSP*, vol. 16, pp. 523-532, 2006.

[15] M. Martorella, "*Novel Approach for ISAR Image Cross-Range Scaling*", *IEEE Trans. on Aerospace and Electronic System*, Vol. 44, No. 1, pp. 281-294, Jan. 2008.

[16] W. G. Carrara, R. S. Goodman, and R. M. Majewski, " *Spotlight Synthetic Aperture Radar Signal Processing Algortithms*", *Norwood*, MA:Artech House, 1995.

[17] S. N. Madsen, " *Estimating The Doppler centroid of SAR Data*", *IEEE Trans. on Aerospace and Electronic System*, Vol. 25, No. 2, pp. 134-140, March 1989.

[18] F. Wong, I and G. Cumming " *A combined SAR Doppler Centroid Estimation Scheme Based upon Signal Phase*", *IEEE Trans. on Geoscience and Remote Sensing*, Vol. 34, No. 3, pp. 696-707, May 1996.

[19] F. Li, D. N. Curlander, and C. Wu, " *Doppler Parameter Estimation for Spaceborne Synthetic-Aperture Radars*", *IEEE Trans. on Geoscience and Remote Sensing*, Vol. 23, No. 1, pp. 696-707, Jan 1985.

[20] J. R. Bennett, I. G. Cumming, P. R. McConnell, and L. Gutteridge " *Features of a generalized digital Synthetic Aperture Radar Processor*", *15th Inter. Synmp. on Remote Sensing of the Environment, Ann Arbor, Michigan, May*.

[21] R. Bamler, " *Doppler Frequency Estimation and the Cramer-Rao Bound*", *IEEE Trans. on Geoscience and Remote Sensing*, Vol. 29, No. 3, pp. 385-390, May. 1991.

[22] D. R. Wehner, " *High Resolution Radar-Second Edition*", *Norwood*, MA:Artech House, 1995.

[23] F. Berizzi, E. Dalle Mese, M. Diani, and M. Martorella, " *High-Resolution ISAR Imaging of Manuvering Targets by Means of the Range Istantaneous Doppler Technique: Modelling and Performance Analysis*", *IEEE Trans. on Image Processing*, Vol. 10, No. 12, pp. 1880-1890, Dec. 2001.

[24] M. Martorella, F. Berizzi, and B. Haywood, " *Contrast maximization based technique for 2-D ISAR autofocusing* ", *IEE Proc. Radar Sonar Navig.*, Vol. 152, No. 4, pp. 253-262, Aug. 2005.

[25] R. Lanari, M. Tesauro, E. Sansosti, and G. Fornaro " *Spotlight SAR Data Focusing Based on a Two-Step Processing Approach*", *IEEE Trans. on Geoscience and Remote Sensing*, Vol. 39, No. 9, pp. 1993-2003, Sept. 2001.

[26] F. Covello, F. Battazza, A. Coletta, G. Manoni, and G. Valentini, " *COSMO-SkyMed Mission Status: Three out of Four Satellites in Orbit*", *Proc. IGARSS09*, Cape Town, South Africa, July 12-17, 2009.

[27] L. Xi, L. Giosui, and J. Ni, " *Autofocusing of ISAR images based on entropy minimization*", *IEEE Trans. on Aerospace and Electronic System*, Vol. 35, No. 4, pp. 1240-1252, Apr. 1999.